RESEARCH PAPER

Computational Validation Of The Therapeutic Potential And Target Interactions Of Wrightia Tinctoria Against Psoriasis-Associated Receptors

Sai Chakith MR[1], Sushma Pradeep[2], Pruthvish Reddy[3], Monika B Premkumar[2], Prithvi Thimmadka[2], Shiva Prasad Kollur[4], Chandan Shivamallu[5*], Anil Kumar K M[6], A M Satish[1*]

[1]*Department of Pharmacology, JSS Medical College, JSS Academy of Higher Education and Research, Mysuru - 570015, Karnataka, India;*
[1]*Department of Cell Biology and Molecular Genetics, Sri Devaraj Urs Academy of Higher Education and Research, Kolar.*
saichakithmr@jssuni.edu.in; amsatish@jssuni.edu.in
[2]*Centre for Digital Health & AI, JSS Medical College & Hospital, JSS Academy of Higher Education and Research, Mysuru – 570 015, Karnataka, India;*
sushmap@jssuni.edu.in; 24plm056@jssuni.edu.in; 25plm016@jssuni.edu.in
[3]*Department of Biotechnology, Acharya Institute of Technology, Bengaluru, Karnataka, India;*
pruthvi19@gmail.com
[4]*School of Physical Sciences, Amrita Vishwa Vidyapeetham, Mysuru Campus, Mysuru – 570 026, Karnataka, India.*
shivachemist@gmail.com
[5]*Department of Biotechnology and Bioinformatics, School of Life Sciences, JSS Academy of Higher Education and Research, Mysuru – 570 015, Karnataka, India;*
chandans@jssuni.edu.in
[6]*Department of Environmental Science, School of Life Sciences, JSS Academy of Higher Education and Research, Mysuru – 570 015, Karnataka, India;*
anilkumarenvi@jssuni.edu.in

ABSTRACT
Psoriasis is a chronic immune-mediated inflammatory skin disorder driven predominantly by the TNF-α/IL-23/IL-17 cytokine axis. Although several biologics effectively target these pathways, their cost and adverse effects necessitate the discovery of safe, plant-derived multi-target modulators. This study employed an integrated computational pipeline to validate the therapeutic potential of Wrightia tinctoria phytochemicals against psoriasis-associated receptors. Network pharmacology (DisGeNET → STRING → Cytoscape/CytoHubba) identified ten inflammation-central hubs: TNF-α, IL-6, IL-17A, IL-22, IL-10, IL-17RA, TGFB1, IL-9, JAK1, and TYK2. HR-LCMS-derived phytochemicals were curated and subjected to ligand preparation, molecular docking, and ADMET analysis. Among forty screened ligands, linoleic acid, β-sitosterol, cycloartenol, and lupeol demonstrated strong affinity toward TNF-α, IL-6, IL-17A, and IL-22 through multiple hydrogen bonds and hydrophobic interactions. ADMET predictions indicated that most phytochemicals showed favorable permeability, low mutagenicity, and acceptable hERG and ClinTox profiles suitable for topical application. Docking interactions suggested a multi-target mechanism resembling biologic immunomodulation. These findings highlight W. tinctoria as a promising source of topical anti-psoriatic agents and provide a mechanistic basis for further molecular dynamics (MD) simulations and preclinical validation..

Keywords: Psoriasis, Wrightia tinctoria, cytokines, IL-6, TNF-α, Computational analysis..
How to cite this article: Chakith MR, Pradeep S, Reddy P, Premkumar MB, Thimmadka P, Kollur SP, Shivamallu C, Kumar KM, Satish AM, Computational Validation Of The Therapeutic Potential And Target Interactions Of Wrightia Tinctoria Against Psoriasis-Associated Receptors..Int J Drug Deliv Technol. 2026;16 (1s): 495-517; DOI: 10.25258/ijddt.16. 495-517
Source of support:. None
Conflict of interest: None

INTRODUCTION

Psoriasis is a chronic, immune-mediated inflammatory skin condition that affects roughly 2-3% of the global population. It is distinguished by erythematous, scaly plaques that appear mostly on the elbows, knees, scalp, and trunk, and it greatly reduces quality of life while being linked to systemic comorbidities such as psoriatic arthritis, cardiovascular problems, and metabolic syndrome [1]. Psoriasis is caused by immune system dysregulation, including abnormal activation of dendritic cells and Th17 lymphocytes. This results in excessive production of pro-inflammatory cytokines such as TNF-α, IL-6, IL-17A, IL-22, and IL-1β. These cytokines promote keratinocyte hyperproliferation and persistent skin inflammation via positive feedback loops involving NF-κB, STAT3, and MAPK [2].

*Author for Correspondence: Sai Chakith MR

.

Despite breakthroughs in biologic medicines that target specific cytokines or immunological checkpoints, current treatments are limited by high cost, systemic immunosuppression, and poor long-term efficacy. This highlights the critical need for alternate, multi-targeted, and safer therapeutic techniques, particularly those amenable for topical application. Medicinal herbs are a promising source of bioactive compounds with immunomodulatory, anti-inflammatory, and skin-repairing properties.

Wrightia tinctoria (Apocynaceae), often known as "Sweet Indrajao," has long been utilized in Ayurvedic and Siddha medicine to treat skin conditions like psoriasis, vitiligo, and eczema [3]. Preliminary phytochemical and pharmacological studies show that its constituents, including triterpenoids (lupeol, friedelin), sterols (β-sitosterol), iridoids (picroside I), and unsaturated fatty acids (linoleic and oleic acids), have anti-inflammatory and antiproliferative properties relevant to psoriatic pathology [4]. However, our molecular understanding of their interactions with disease-associated targets remains limited.

Network pharmacology, an emerging systems biology technique, enables comprehensive mapping of multi-component, multi-target interactions, making it well-suited for research on complex disorders such as psoriasis [5]. When combined with molecular docking and ADMET (absorption, distribution, metabolism, excretion, and toxicity) predictions, *in silico* techniques provide a rapid and cost-effective approach to identify and validate candidate therapies with favourable pharmacokinetic and safety profiles [6].

The goal of this study was to computationally assess *Wrightia tinctoria's* therapeutic potential using network pharmacology, molecular docking, and ADMET profiling. Forty compounds discovered through HR-LCMS analysis of the plant extract were docked with ten psoriasis-associated cytokines and signaling proteins. The ligands' drug-likeness and topical applicability were assessed using the ADMET and BOILED-Egg models, respectively. This integrated method discovered high-performing chemicals, including β-sitosterol and linoleic acid, with strong cytokine-binding affinities, excellent safety profiles, and promise for topical anti-psoriatic use.

MATERIALS AND METHODS

2.1 Network Pharmacology and Target Selection

Genes associated with plaque psoriasis (Disease ID: C0406317) were retrieved from the DisGeNET database and used to construct a disease–gene network [7]. Protein–protein interaction (PPI) data for these psoriasis-related genes were obtained from STRING v11.5 (confidence score ≥ 0.7) and imported into Cytoscape v3.9.1. The CytoHubba plugin (MCC algorithm) was applied to identify the top 10 hub proteins in the network [8]. These hubs were interpreted as central nodes driving psoriatic pathology.

2.2 Ligand Preparation

Phytochemical constituents of *W. tinctoria* leaves were identified by high-resolution LC–MS (ethanolic extract). A library of 40 confirmed compounds was compiled, and their 2D structures or SMILES strings were obtained from PubChem. Ligand preparation was performed in Schrödinger's Maestro (LigPrep) using the OPLS4 force field. All structures were energy-minimized and protonated at physiological pH (7.0 ± 0.5); relevant stereochemistry was retained and low-energy 3D conformers were generated for each ligand [9].

2.3 Protein Preparation

Crystal structures (or highest-quality available structures) of the ten psoriasis-associated protein targets – TNF-α, IL-6, IL-17A, IL-10, IL-22, TGF-β1, IL-9, IL-17RA, JAK1, and TYK2 – were retrieved from the Protein Data Bank. Each protein structure was prepared using the Protein Preparation Wizard: bond orders were assigned, hydrogen atoms added, protonation states optimized for pH ~7, crystallographic water molecules beyond 5 Å from binding pockets were removed, and missing side-chains or loops were modeled if necessary. Finally, a restrained energy minimization (OPLS4 force field) was applied to relieve steric clashes and optimize the protein structures for docking. Biologically relevant oligomeric assemblies (e.g. the TNF-α trimer, IL-17A dimer) were preserved to maintain correct binding interfaces [10].

2.4 Molecular Docking

Molecular docking simulations were conducted for all 40 phytochemical ligands against the panel of 10 psoriasis-related protein targets. Receptor grid maps were defined at the active or ligand-binding sites of each protein. Glide (Schrödinger) was used in Standard Precision (SP) mode to dock each ligand into each protein's binding site. For each ligand–protein pair, the best-ranked binding pose (lowest Glide docking score) was recorded. Key protein–ligand interactions including hydrogen bonds, hydrophobic contacts, and π–π stacking were analyzed for the top poses [8]. This docking protocol enabled a comparative assessment of how different *W. tinctoria* phytochemicals might interact with critical cytokines and signaling receptors implicated in psoriasis.

2.5 ADMET Prediction

The pharmacokinetic and toxicity profiles of the phytochemicals were predicted using the ADMET-AI platform. A range of *in silico* ADMET parameters was evaluated for each compound: human intestinal absorption (HIA_Hou index for oral bioavailability), aqueous solubility (logS), blood–brain barrier (BBB) penetration probability, CYP3A4 inhibition likelihood, predicted biological half-life, hERG potassium channel inhibition probability, Ames mutagenicity, and an integrated toxicity risk (ClinTox). Each compound was assessed against standard drug-likeness criteria (Lipinski's Rule of Five) and classified as favorable, unfavorable/Review based on its overall ADMET profile for potential topical use [11]. A BOILED-Egg model was also generated to visualize the passive gastrointestinal absorption and BBB permeation tendencies of selected compounds (in particular, major fatty acids) via their position in the physicochemical space of polarity (TPSA) and lipophilicity (WLOGP) [12].

RESULTS AND DISCUSSION

3.1. Network pharmacology analysis

3.1.1. Network Pharmacology and Target Selection

Using DisGeNET (Disease ID: C0406317), a disease–gene visualization was generated to overview genes linked to plaque psoriasis. The plot shows *Plaque psoriasis* as the central node, with radiating edges to immune regulators and cytokines, including IL6, IL17A, TNF-α, TYK2, IL23A, IL37, IL34, HLA-C, AHR, JAK1, among others, highlighting the dominance of interleukin signalling and antigen-presenting genes within psoriatic biology (**Figure 1**)

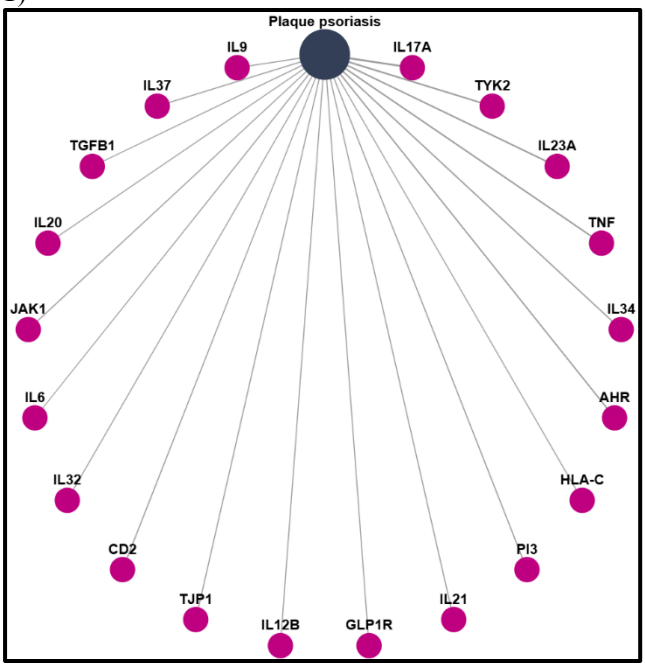

.

Figure 2: STRING-derived PPI network visualized in Cytoscape. Warmer node colors (red→orange→yellow) indicate increasing CytoHubba MCC centrality; cooler lavender nodes are less central. Dense interconnections among TNF-α, IL6, IL17A, IL10, IL22, TGFB1, IL9, JAK1, TYK2, IL17RA form the functional core.

The integrated network analysis of STRING and Cytoscape further elucidated the intricate immune signaling landscape underlying psoriasis. Quantitative topological evaluation using CytoHubba metrics—MCC, closeness centrality, edge count, and betweenness centrality—revealed that TNF-α and IL-6 occupy the most central positions within the psoriatic interactome, followed closely by IL-17A, IL-10, and IL-22 (**Figure 3**). These cytokines form the core of the inflammatory cascade, coordinating keratinocyte activation, T-cell differentiation, and cytokine amplification loops. The inclusion of kinase regulators JAK1 and TYK2, as well as immune markers such as IL-9 and IL-17RA, emphasizes the convergence of Th17 and JAK-STAT signaling pathways in disease pathogenesis.

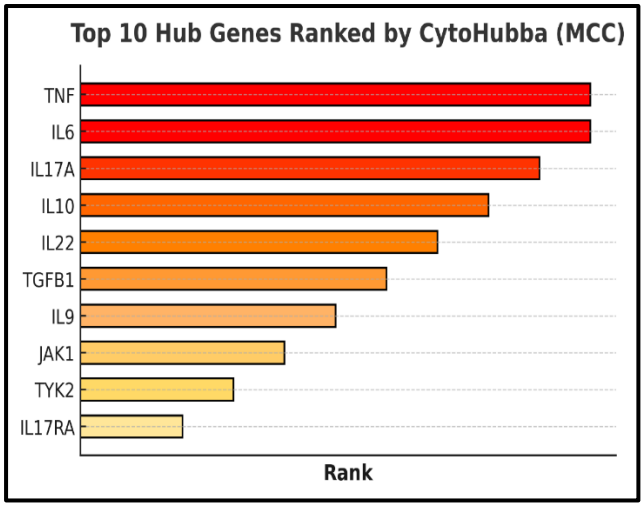

Figure 3: Top-10 interactive genes ranked by CytoHubba (MCC). The ranking emphasizes TNF-α, IL6, and IL17A as highest-centrality nodes, followed by IL10, IL22, TGFB1, IL9, JAK1, TYK2, IL17RA.

The top ten hub genes obtained from Cytoscape analysis are summarized in **Table 1**.

Table 1: Top 10 hub genes involved in psoriasis inflammation ranked by closeness centrality, edge count, and betweenness centrality metrics obtained from Cytoscape analysis.

Gene Name	MCC Score	Closeness Centrality	Edge Count	Betweenness Centrality
TNF-α	503068	1.000000	26	1.000000
IL6	503068	1.000000	26	1.000000
IL17A	502104	0.924528	22	0.427889
IL10	501624	0.943396	23	0.514222
IL22	501120	0.867925	19	0.229222
TGFB1	500828	0.867925	18	0.106000
IL9	500276	0.830189	17	0.203352
JAK1	500152	0.830189	16	0.196162
TYK2	499986	0.792453	15	0.159595
IL17RA	499836	0.754717	14	0.090826

Molecular Interaction Studies

Screening of Ligands

The ligand panel for the study was exclusively derived from the ethanolic leaf extract of *Wrightia tinctoria*. HR-LCMS profiled the extract, and the resulting confirmed plant metabolites were curated into a candidate set for *in-silico* evaluation. For each shortlisted phytoconstituent, the canonical structure and SMILES were retrieved from

PubChem, then prepared for docking using the standard workflow (physiological protonation, tautomer/ionisation state enumeration, stereoisomer consideration where relevant, and OPLS4 energy minimisation) to yield chemically realistic 3D conformers. The top 40 phytochemicals with the smiles are listed in **Table 2**.

Table 2: List of 40 phytochemicals identified from *Wrightia tinctoria* extract used for molecular docking and ADMET analysis.

Sl.no	Name	Smiles	Structure
	3aR,4R,5R,6aS)-5-Hydroxy-4-{(3R)-3-hydroxy-4-[3-(trifluoromethyl)phenoxy]but-1-en-1-yl}hexahydro-2H-cyclopenta[b]furan-2-one	C1[C@H]([C@@H]([C@@H]2[C@H]1OC(=O)C2)C=C[C@H](COC3=CC=CC(=C3)C(F)(F)F)O)O	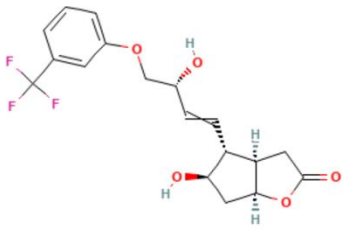
	β-Sitosterol	CC[C@H](CC[C@@H](C)[C@H]1CC[C@@H]2[C@@]1(CC[C@H]3[C@H]2CC=C4[C@@]3(CC[C@@H](C4)O)C)C)C(C)C	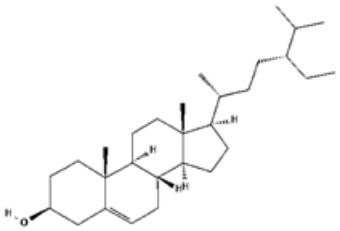
	Dodecyltriphenylphosphonium	CCCCCCCCCCCC[P+](C1=CC=CC=C1)(C2=CC=CC=C2)C3=CC=CC=C3	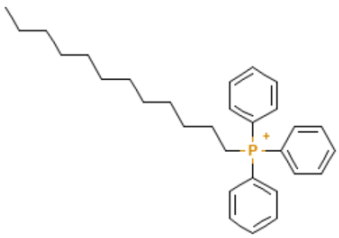
	1-(1,2-Dioctanoylphosphatidyl)inositol_	CCCCCCCC(=O)OC[C@H](COP(=O)([O-])O[C@@H]1[C@H](O)[C@H](OP(=O)([O-])[O-])[C@@H](O)[C@H](O)[C@H]1O)OC(=O)CCCCCCC	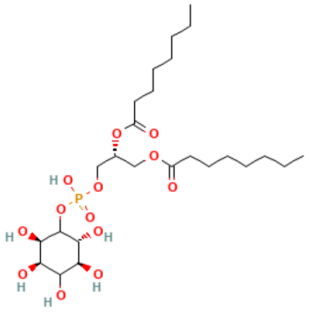
	Friedelin	C[C@H]1C(=O)CC[C@@H]2[C@@]1(CC[C@H]3[C@]2(CC[C@@]4([C@@]3(CC[C@@]5([C@H]4CC(CC5)(C)C)C)C)C)C)C	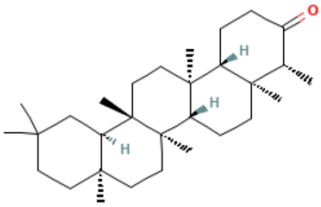

	Cornuside	COC(=O)C1=CO[C@@H]([C@H]([C@H]1CCOC(=O)C2=CC(=C(C(=C2)O)O)O)C=C)O[C@H]3[C@@H]([C@H]([C@@H]([C@H](O3)CO)O)O)O)O	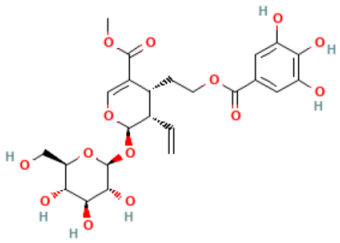
	Peonidin cation	COC1=C(C=CC(=C1)C2=[O+]C3=CC(=CC(=C3C=C2O)O)O)O	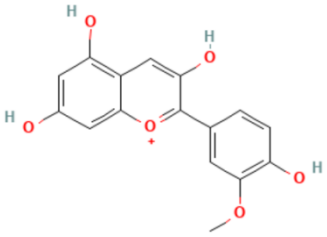
	Peonidin 3-galactoside cation	CC(=O)OC[C@@H]1[C@@H]([C@@H]([C@H](C(O1)OC2=CC3=C(C=C(C=C3[O+]=C2C4=CC(=C(C=C4)O)OC)O)O)O)O)O	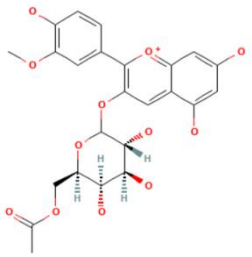
	Sesamoside	C[C@@]12[C@H]3[C@@H](OC=C([C@]3([C@@H]([C@@H]1O2)O)O)C(=O)OC)O[C@H]4[C@@H]([C@H]([C@@H]([C@H](O4)CO)O)O)O)O	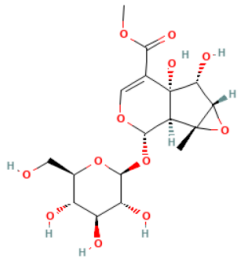
	15(R),19(R)-Hydroxyprostaglandin F2.alpha.	C[C@H](CCC[C@H](/C=C/[C@H]1[C@@H](C[C@@H]([C@@H]1C/C=C\CCCC(=O)O)O)O)O)O	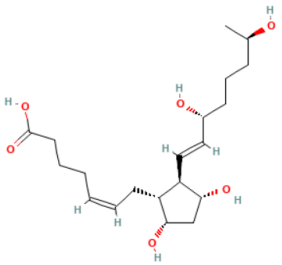
	Cycloartenol	C[C@H](CCC=C(C)C)[C@H]1CC[C@@]2([C@@]1(CC[C@]34[C@H]2CC[C@@H]5[C@]3(C4)CC[C@@H](C5(C)C)O)C)C	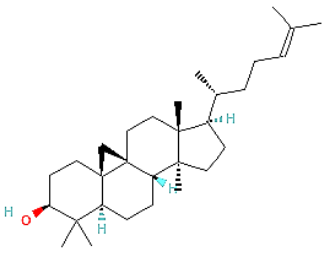

	17a-Nandrolone	C[C@]12CC[C@H]3[C@H]([C@@H]1CC[C@H]2O)CCC4=CC(=O)CC[C@H]34	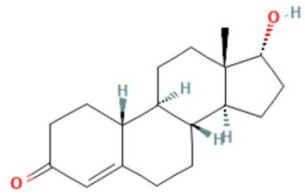
	Dodecamethylcyclohexasiloxane	C[Si]1(O[Si](O[Si](O[Si](O[Si](O[Si](O1)(C)C)(C)C)(C)C)(C)C)(C)C)C	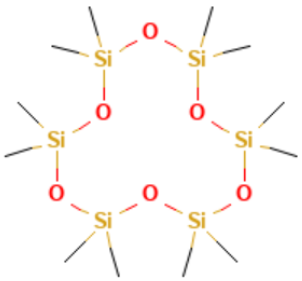
	16,16-Dimethylprostaglandin D2	CCCCC(C)(C)[C@@H](/C=C/[C@@H]1[C@H]([C@H](CC1=O)O)C/C=C\CCCC(=O)O)O	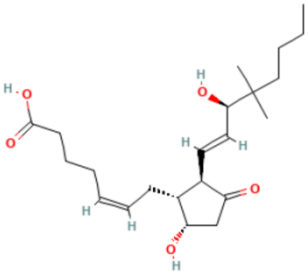
	Mono-2-ethylhexyl phthalate	CCCCC(CC)COC(=O)C1=CC=CC=C1C(=O)O	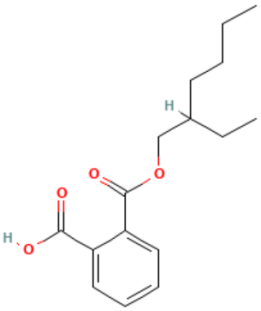
	Qingyangshengenin	CC(=O)C1(CCC2(C1(C(CC3C2(CC=C4C3(CCC(C4)O)C)O)OC(=O)C5=CC=C(C=C5)O)C)O)O	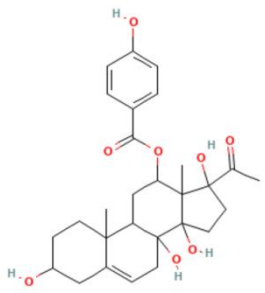

	Vincamone	CC[C@@]12CCCN3[C@@H]1C4=C(CC3)C5=CC=CC=C5N4C(=O)C2	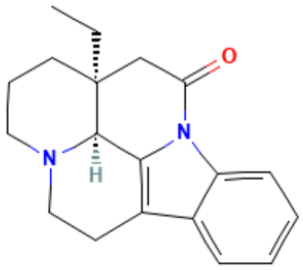
	Pinolenic acid ethyl ester	CCCCC/C=C\C/C=C\CC/C=C\CCCC(=O)OCC	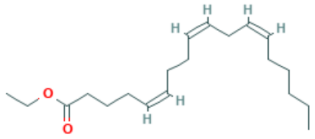
	Nigerose	C([C@@H]1[C@H]([C@@H]([C@H]([C@H](O1)O[C@H]2[C@@H]([C@H](OC([C@@H]2O)O)CO)O)O)O)O)O	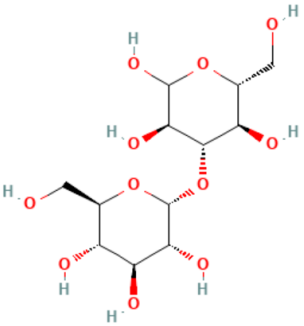
	Linoleic acid	CCCCC/C=C\C/C=C\CCCCCCCC(=O)O	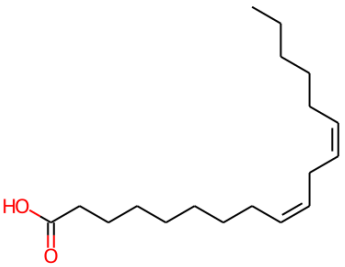
	10E,12Z-octadecadienoic acid	CCCCC/C=C\C=C\CCCCCCCCC(=O)O	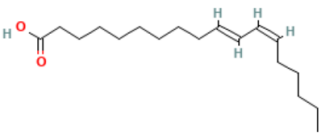
	15(R)-15-Methylprostaglandin F2.alpha. methyl ester	CCCCC[C@](C)(/C=C/[C@H]1[C@@H](C[C@@H]([C@@H]1C/C=C\CCCC(=O)OC)O)O)O	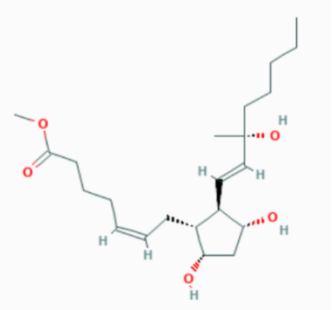

	Oleoside 11-methyl ester	C/C=C/1\[C@@H](C(=CO[C@H]1O[C@H]2[C@@H]([C@H]([C@@H]([C@H](O2)CO)O)O)O)C(=O)OC)CC(=O)O	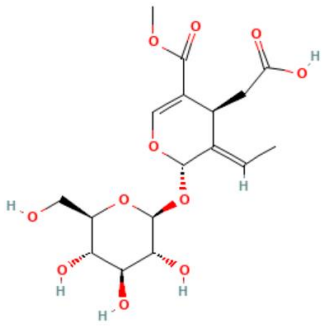
	Oleic acid	CCCCCCCC/C=C\CCCCCCCC(=O)O	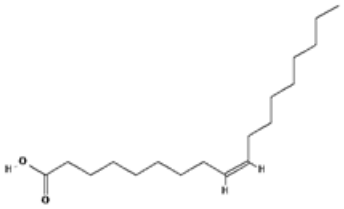
	Linderane	C/C/1=C\CC[C@@]23[C@@H](O2)[C@H](C4=C(C1)OC=C4C)OC3=O	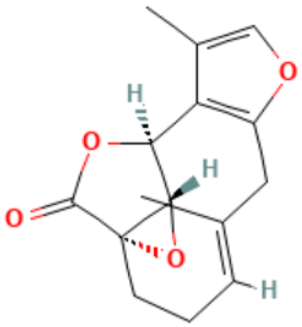
	Isopimaric acid	C[C@@]1(CC[C@H]2C(=CC[C@@H]3[C@@]2(CCC[C@@]3(C)C(=O)O)C)C1)C=C	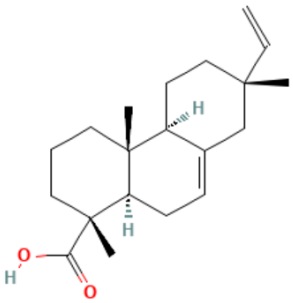
	Lupeol	CC(=C)[C@@H]1CC[C@]2([C@H]1[C@H]3CC[C@@H]4[C@]5(CC[C@@H](C([C@@H]5CC[C@]4([C@@]3(CC2)C)C)(C)C)O)C)C	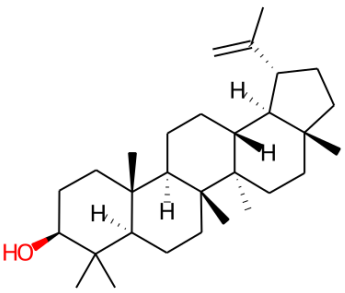

	Tricaprylin	CCCCCCCC(=O)OCC(COC(=O)CCCCCCC)OC(=O)CCCCCCC	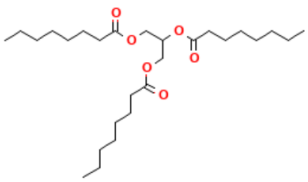
	Bicyclo-prostaglandin E1	CCCCC1[C@H]2CC(=O)C([C@H]2CCC1=O)CCCCCCC(=O)O	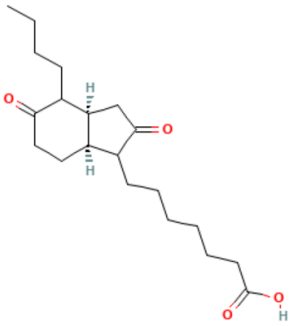
	3-Methoxylimaprost	CCCC[C@H](C)C[C@@H](/C=C/[C@H]1[C@@H](CC(=O)[C@@H]1CCCCC(CC(=O)O)OC)O)O	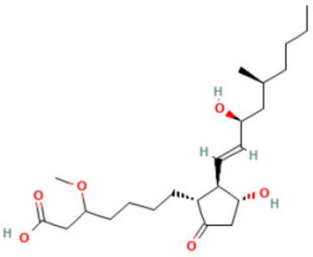
	Hyodeoxycholic acid	C[C@H](CCC(=O)O)[C@H]1CC[C@@H]2[C@@]1(CC[C@H]3[C@H]2C[C@@H]([C@H]4[C@@]3(CC[C@H](C4)O)C)O)C	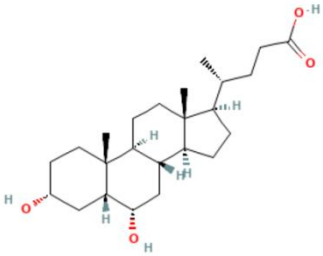
	Isoalantolactone	C[C@]12CCCC(=C)[C@@H]1C[C@H]3[C@@H](C2)OC(=O)C3=C	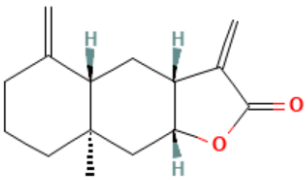
	Picroside I	C1=CC=C(C=C1)/C=C/C(=O)OC[C@@H]2[C@H]([C@@H]([C@H]([C@@H](O2)O[C@H]3[C@H]4[C@@H](C=CO3)[C@@H]([C@H]5[C@@]4(O5)CO)O)O)O)O	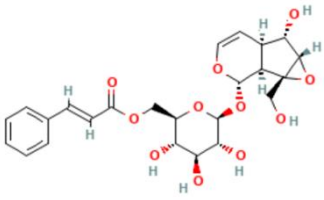
	Citrinin	C[C@@H]1[C@H](OC=C2C1=C(C(=C(C2=O)C(=O)O)O)C)C	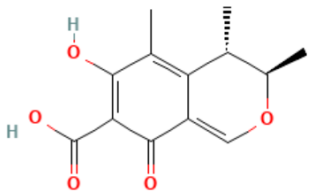

	Ethyl Linoleate	CCCCC/C=C\C/C=C\CCCCCCCC(=O)OCC	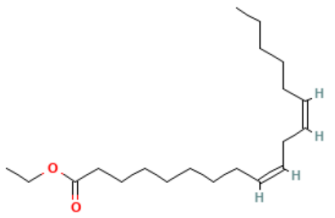
	Acid Violet 9	CC1=CC=CC=C1NC2=CC3=C(C=C2)C(=C4C=CC(=CC4=[O+]3)NC5=C(C=C(C=C5)S(=O)(=O)[O-])C)C6=CC=CC=C6C(=O)O.[Na+]	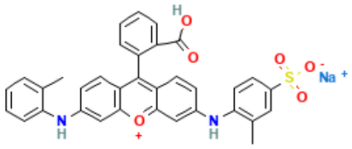
	Quinupramine	C1CN2CCC1C(C2)N3C4=CC=CC=C4CCC5=CC=CC=C53	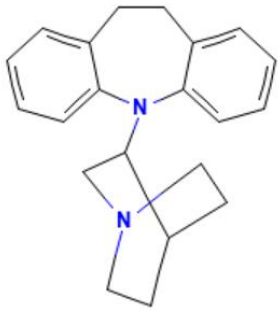
	Brefeldin A	C[C@H]1CCC/C=C/[C@@H]2C[C@@H](C[C@H]2[C@@H](/C=C/C(=O)O1)O)O	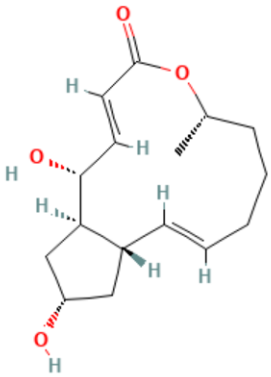
	4-(1-Phenylcyclohexyl)morpholine	C1CCC(CC1)(C2=CC=CC=C2)N3CCOCC3	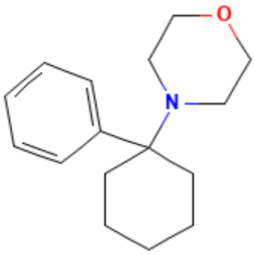
	Hexamethylcyclotrisiloxane	C[Si]1(O[Si](O[Si](O1)(C)C)(C)C)C	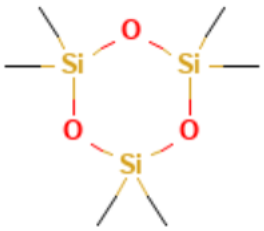

Molecular Docking

All 40 *W. tinctoria*-derived ligands were docked against each of the 10 selected protein targets. The docking simulations yielded Glide scores for each ligand–target pair, reflecting the predicted binding affinity. Overall, the majority of phytochemicals formed at least moderate interactions with one or more psoriasis-related targets, suggesting a potential multitarget therapeutic effect. Notably, certain compounds stood out with consistently high binding affinities across multiple cytokines. Linoleic acid (an unsaturated fatty acid) and β-sitosterol (a phytosterol) emerged as top-performing ligands, exhibiting low docking scores (high affinity) and extensive interaction networks within the binding sites of TNF-α, IL-6, IL-17A, IL-10, and IL-22. These two phytochemicals were among an initial set of top ten ligands ranked by docking score, from which they were selected for detailed analysis. Other triterpenoids such as cycloartenol and lupeol also showed strong binding to several cytokines, indicating that *W. tinctoria*'s bioactive components tend to target inflammatory mediators synergistically. The corresponding docking scores, hydrogen bond details, and key interacting residues for these top ligands are summarized in **Table 2.**

Table 2: Docking results of selected *W. tinctoria* phytochemicals and reference anti-psoriatic drugs against key cytokine targets. For each ligand, the number of hydrogen bonds (H-bonds) with each protein and the key interacting amino acid residues are listed, along with the Glide docking score for the best pose

Sl no	Ligand	Protein	H bond	Amino acid
1	Linoleic acid	TNF-α	7	GLN B:61, SER B:60, GLY A:122, TYR A:119, TYR C:119, GLY C:121, ILE A:155
		IL6	6	ARG 104, ASP 160, THR 43, LYS 46, SER 47, PHE 105
		IL17A	8	GLN F:82, PRO C:113, VAL C:115, VAL C:205, VAL C:110, LYS F:19, TYR 60
		IL10	7	VAL 124, TYR 149, GLU 142, ILE 145, PHE 146, PHE 128, LEU 131
		IL22	5	ALA A:23, GLU A:26, ALA A:121, THR A:20, ARG A:24
2	Oleic acid	TNF-α	4	GLY A:122, GLN B:61, SER B:60, VAL A:123
		IL6	-	-
		IL17A	4	TYR 60, ARG 59, SER 61, PRO 62
		IL10	-	-
		IL22	4	GLU A:26, ARG A:24, ASN A:124, ALA A:121
3	β-Sitosterol	TNF-α	6	TYR A:119, GLN B:61, TYR C:59, GLY C:122, LEU A:157, GLY C:122
		IL6	9	GLU 42, GLU 106, SER 107, SER 108, ASN 48, GLN 156, ASP 160, TRP 157
		IL17A	7	ALA C:112, SER C:114, THR F:69, ILE F:51, VAL F:68, ALA C:111, GLY C:200
		IL10	6	GLU 142, ALA 139, PHE 143, ILE 145, GLY 135, TYR 149
		IL22	8	GLU A:129, LYS A:125, THR A:31, GLU A:26, ALA A:23, LYS D:125, ASN A:124, ARG A:24
4	Cycloartenol	TNF-α	-	-
		IL6	-	-
		IL17A	8	ARG 108, ALA 111, ALA 72, ILE 70, PRO 113, LEU 201, GLY 66, VAL 68
		IL10	6	PHE 146, ILE 145, ALA 139, LYS 138, TYR 149, LEU 131
		IL22	5	LYS A:125, THR A:31, GLY A:128, ALA A:121, ASP A:118

5	Lupeol	TNF-α	-	-
		IL6	5	SER 107, GLU 106, GLU 42, GLN 156, ARG 104
		IL17A	6	THR 136, VAL 115, TYR 60, SER 202, ALA 112, PHE 116
		IL10	-	-
		IL22	5	GLY A:128, GLU A:129, LYS A:125, THR A:31, ALA A:121
6.	Apremilast	TNF-α	-	-
		IL6	1	ASP 160
		IL17A	3	LYS C:207, TYR F:60, VAL C:115
		IL10	-	-
		IL22	1	LYS D:125, ARG D:24
7	Tapinarof	TNF-α	1	TYR C:119
		IL6	1	GLU 106,
		IL17A	1	VAL C:110
		IL10	1	GLU 142
		IL22	2	GLY A:128, THR A:13
8	Roflumilast	TNF-α	-	-
		IL6	1	ASP 160
		IL17A	1	ASN C:138
		IL10	1	GLU 142,
		IL22	1	LYS A:125
9	Methotrexate	TNF-α	2	TYR C:119
		IL6	2	SER 107
		IL17A	5	TYR F:60, THR D:136, THR D:140, GLN F:82
		IL10	2	GLY 135
		IL22	6	GLY A:128 LYS A:125, THR D:31, LYS D:125

Based on docking scores, hydrogen-bonding interactions, and binding-site complementarity, several phytocompounds demonstrated strong interactions with the selected cytokines. Among these, Linoleic acid and β-Sitosterol were identified as the top candidates. These two compounds were selected from an initial set of ten based on superior docking scores, interaction profiles, and chemical diversity across major phytocompounds. And Methotrexate is used as a reference molecule, its interaction is also compared with the phytocompound interaction

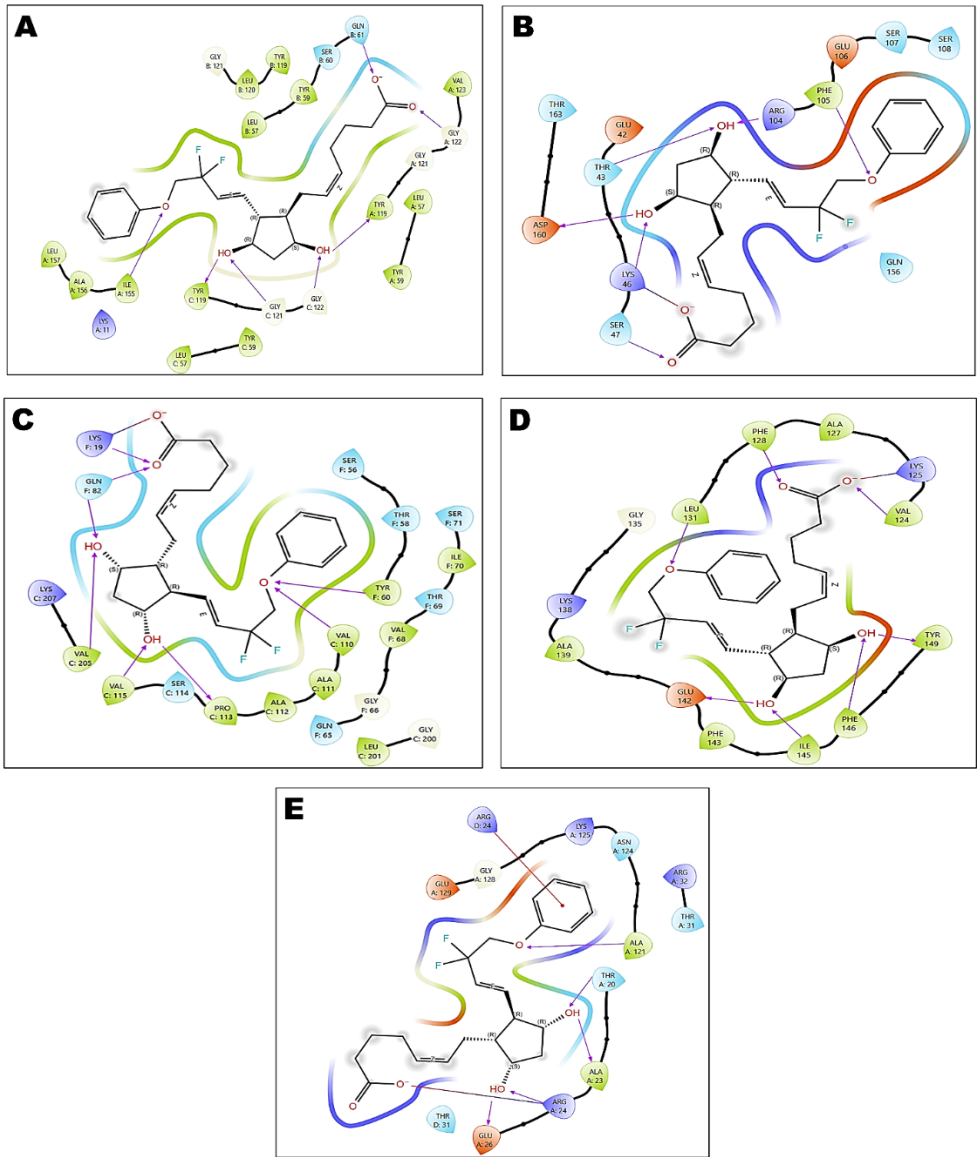

Figure 4: 2D docking interactions of Linoleic acid with the target proteins: (A) TNF-α, (B) IL-6, (C) IL-17A, (D) IL-10, and (E) IL-22.

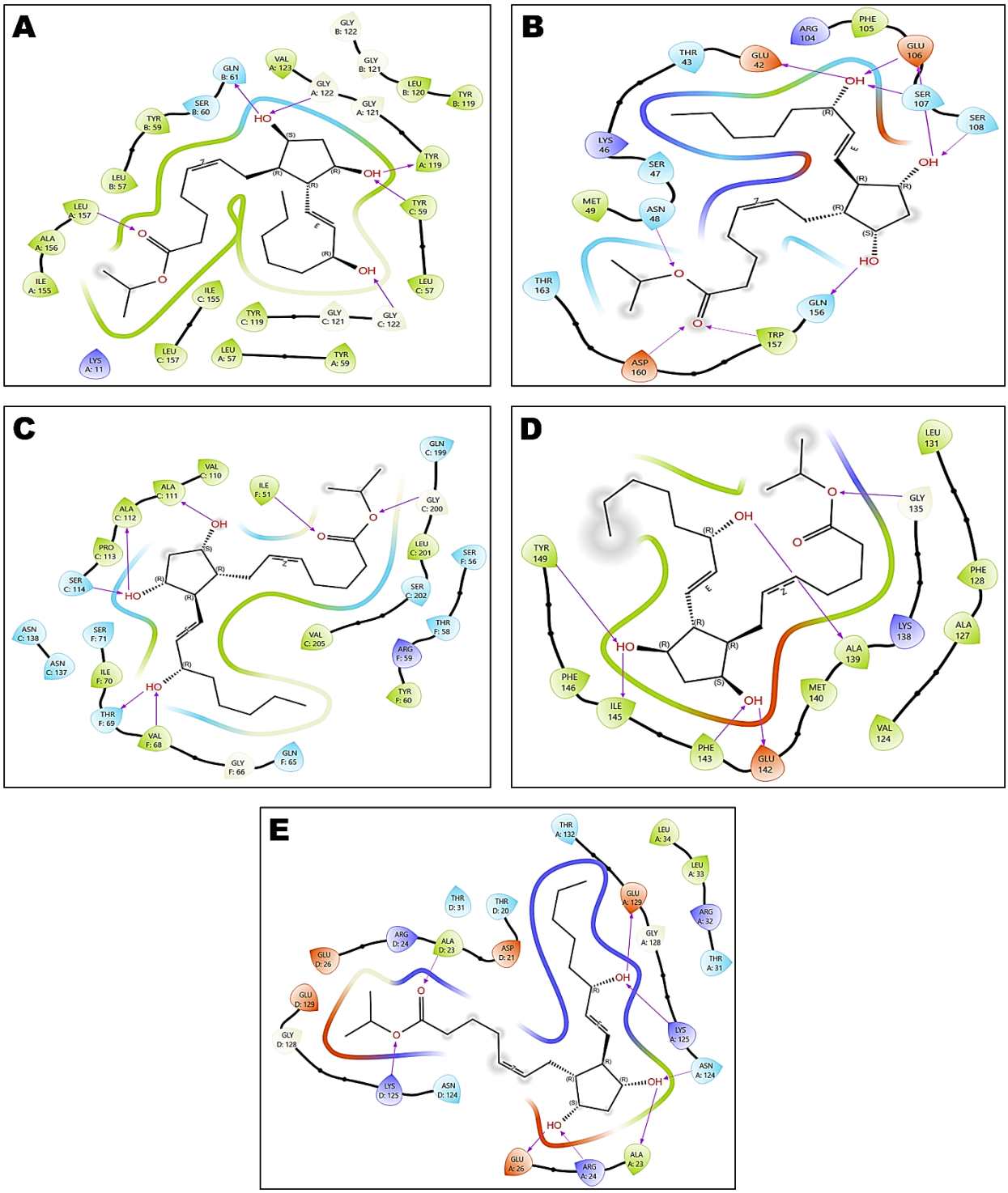

Figure 5: 2D docking interactions of β-Sitosterol with the target proteins: (A) TNF-α, (B) IL-6, (C) IL-17A, (D) IL-10, and (E) IL-22.

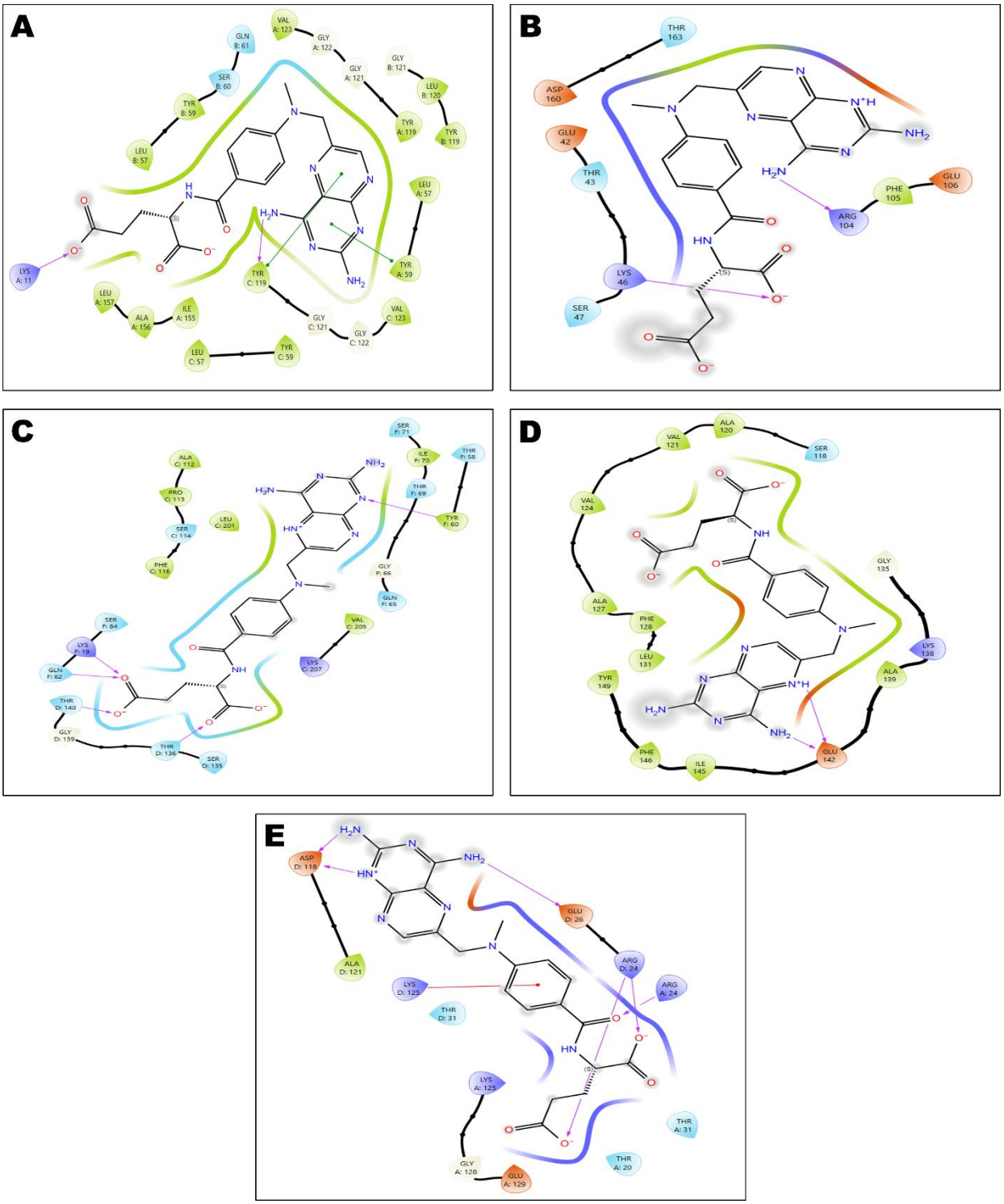

Figure 6: 2D docking interactions of standard drug Methotrexate with the target proteins: (A) TNF-α, (B) IL-6, (C) IL-17A, (D) IL-10, and (E) IL-22

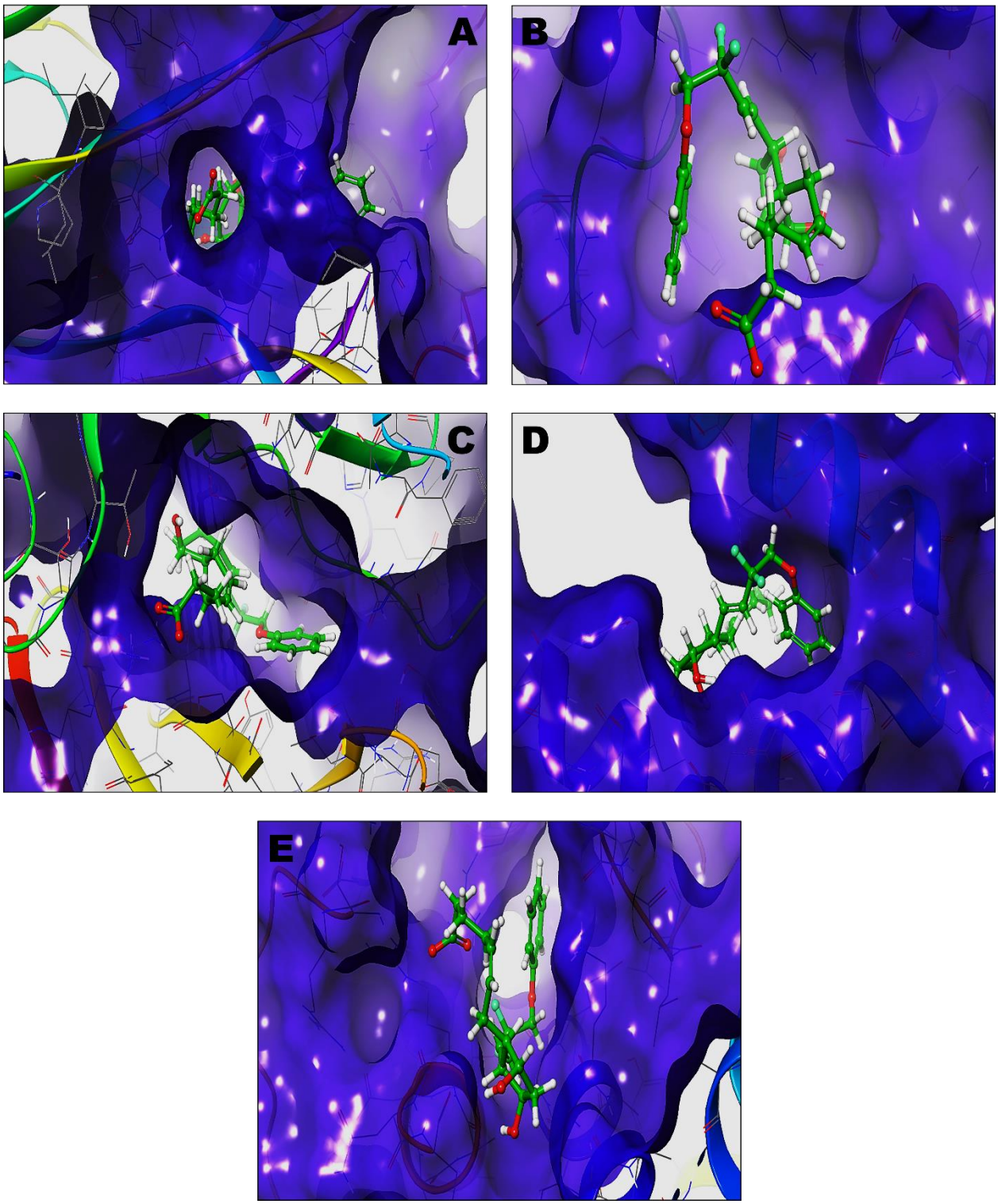

Figure 7: 3D docking interactions of Linoleic acid with target proteins: (A) TNF-α, (B) IL-6, (C) IL-17A, (D) IL-10, and (E) IL-22.

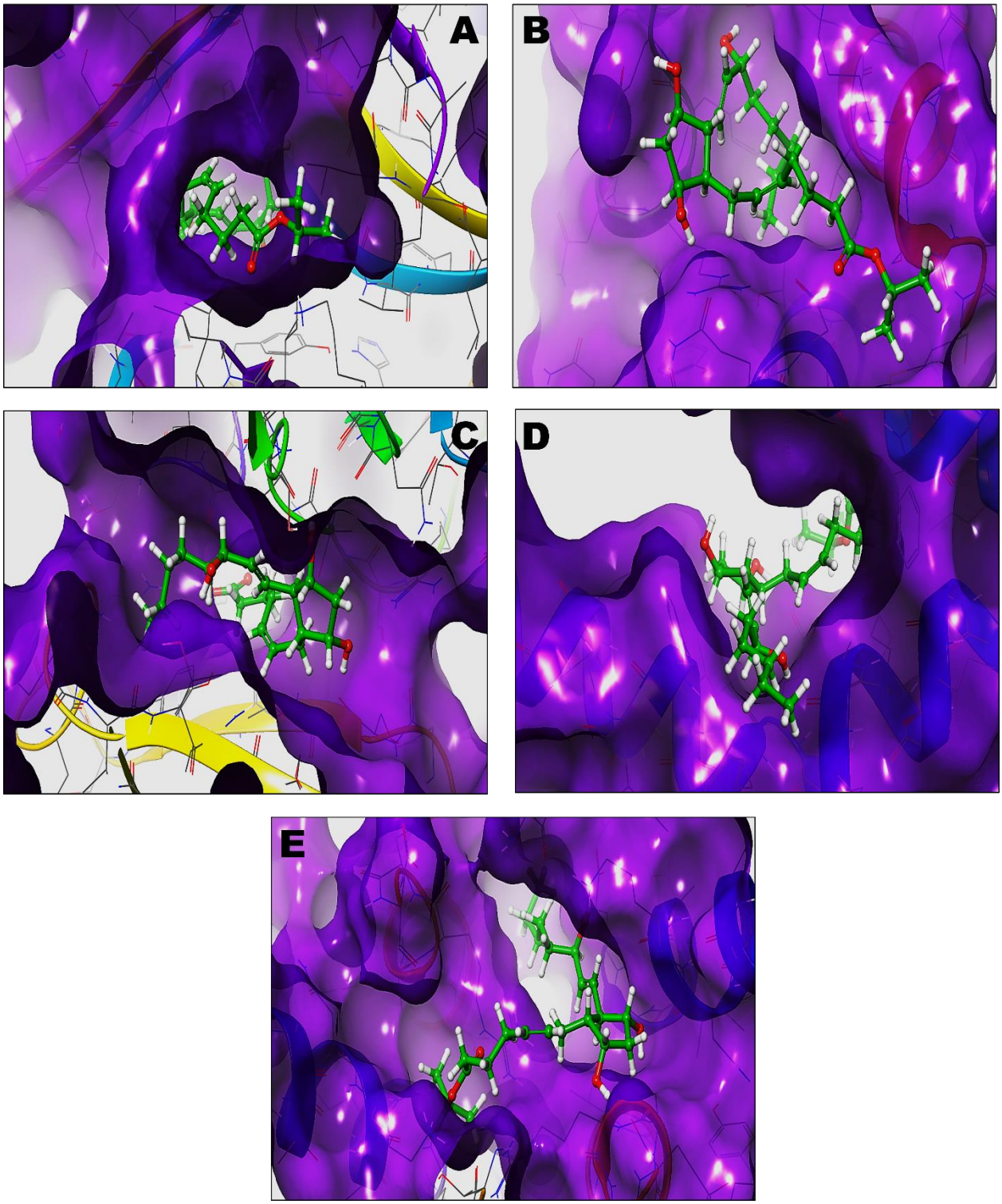

Figure 8: 3D docking interactions of β-Sitosterol with the target proteins: (A) TNF-α, (B) IL-6, (C) IL-17A, (D) IL-10, and (E) IL-22

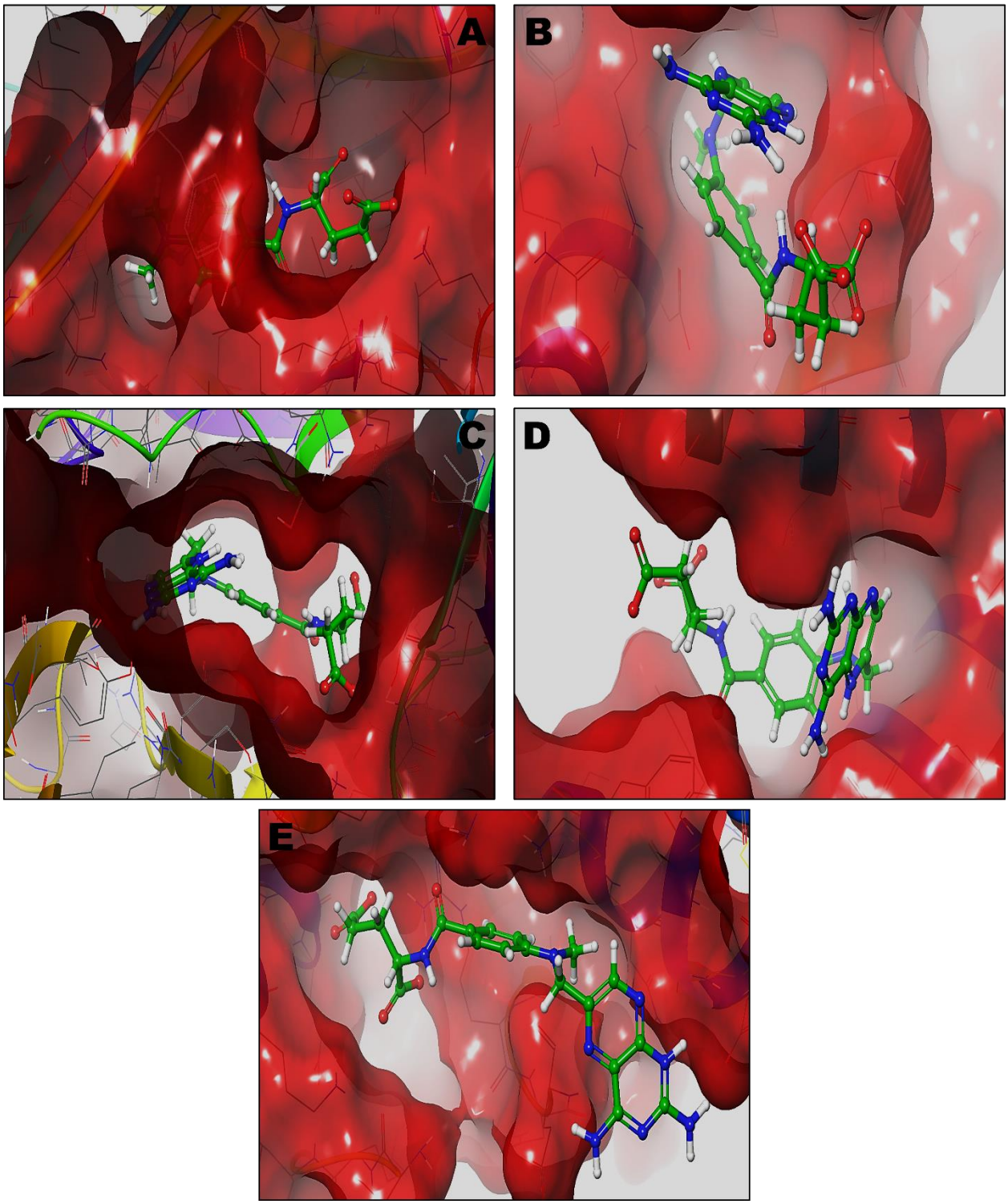

Figure 9: 3D docking interactions of standard drug Methotrexate with the target proteins: (A) TNF-α, (B) IL-6, (C) IL-17A, (D) IL-10, and (E) IL-22

Docking scores suggest that Linoleic acid and β-Sitosterol may act through multi-target cytokine modulation, particularly IL-6 and IL-17A, which are central to psoriatic inflammation [17]. The multitarget interaction profile mirrors the mechanism of action of current biologics, offering a promising therapeutic alternative via oral small molecules.

ADMET Profile of *Wrightia tinctoria* Extract Compounds

ADMET Profiling of Selected Ligands

In-silico ADMET screening performed on 40 phytochemicals from *Wrightia tinctoria* to assess their pharmacokinetic suitability and safety for anti-psoriatic drug development. Each compound was evaluated for oral bioavailability, aqueous solubility, blood–brain barrier (BBB) penetration, cytochrome P450 3A4 (CYP3A4) inhibition, predicted half-life, hERG

channel blocking, Ames mutagenicity, and overall clinical toxicity (ClinTox). A summary of the results is provided in **Table 3.**

Among the screened compounds, β-sitosterol and linoleic acid emerged as the most promising based on their balanced ADMET profiles and favorable pharmacological potential. β-sitosterol showed excellent intestinal absorption (0.998), moderate water solubility (log S = –4.60), and a safe toxicological profile with low mutagenicity (0.183), moderate half-life, and a low ClinTox score (0.096). Though it had moderate BBB permeability (0.748) and a mid-range CYP3A4 inhibition value (0.619), its overall risk for systemic toxicity was low. Being a phytosterol with established anti-inflammatory properties and favorable membrane interaction characteristics, it shows strong topical potential for psoriasis management. Linoleic acid, a naturally occurring polyunsaturated fatty acid, also demonstrated high oral absorption (1.000) and significant skin permeability properties. Despite poor aqueous solubility (log S = –5.53) and elevated BBB penetration (0.943) and CYP3A4 inhibition (0.864) probabilities, its toxicity risk scores remained low (mutagenicity = 0.262, ClinTox = 0.048). Its presence in the BOILED-Egg yellow region indicates high passive permeability and potential for effective dermal uptake—desirable traits for topical delivery. Linoleic acid's known role in restoring skin barrier function and modulating inflammatory responses supports its inclusion in further validation studies. While several compounds (e.g., lupeol, friedelin, 10E,12Z-octadecadienoic acid) also performed well, linoleic acid and β-sitosterol collectively balanced **absorption, safety, and dermatological relevance**, making them top candidates for continued investigation in psoriasis-focused drug development.

Table 3: ADMET properties of all 40 phytochemicals, including oral bioavailability, solubility, blood-brain barrier penetration, CYP3A4 inhibition, half-life, hERG blocking potential, mutagenicity, and ClinTox scores

Sl. No	Ligand	Oral Bioavailability	Solubility (log mol/L)	BBB Penetration	CYP3A4 Inhibition	Half-life (hr)	hERG Blocking	Mutagenicity	ClinTox	Suitability
1	3aR,4R,5R,6aS)-5-Hydroxy-4-{(3R)-3-hydroxy-4-[3-(trifluoromethyl)phenoxy]but-1-en-1-yl}hexahydro-2H-cyclopenta[b]furan-2-one	1	-3.186	0.975	0.266	-7.07	0.622	0.412	0.278	Favourable
2	β-Sitosterol	0.998	-4.599	0.748	0.619	-7.96	0.476	0.183	0.096	Favourable
3	Dodecyltriphenylphosphonium	0.953	-5.906	0.319	0.097	127.97	0.919	0.036	0.011	Favourable
4	1-(1,2-Dioctanoylphosphatidyl)inositol_	0.068	-2.551	0.449	0.029	6.07	0.507	0.024	0.023	Unfavourable/Review
5	Friedelin	0.995	-6.408	0.949	0.018	18.51	0.744	0.013	0.014	Favourable
6	Cornuside	0.291	-3.212	0.166	0.076	-10.71	0.53	0.519	0.169	Unfavourable/Review
7	Peonidin cation	0.999	-3.258	0.146	0.741	-15.72	0.582	0.31	0.034	Favourable
8	Peonidin 3-galactoside cation	0.684	-3.57	0.164	0.055	16.29	0.741	0.467	0.308	Favourable
9	Sesamoside	0.465	-0.676	0.545	0.002	4.62	0.193	0.086	0.159	Unfavourable/Review
10	15(R),19(R)-Hydroxyprostaglandin F2.alpha.	0.796	-1.847	0.393	0.009	-9.82	0.042	0.045	0.1	Favourable
11	Cycloartenol	0.999	-5.988	0.8	0.153	20.57	0.559	0.223	0.128	Favourable

12	17a-Nandrolone	1	-3.346	0.136	0.009	8.39	0.065	0.004	0.004	Favourable
13	Dodecamethylcyclohexasiloxane	0.999	-7.531	0.993	0.005	1.32	0.328	0.326	0.004	Favourable
14	16,16-Dimethylprostaglandin D2	0.988	-3.375	0.627	0.053	-20.98	0.033	0.124	0.114	Favourable
15	Mono-2-ethylhexyl phthalate	0.999	-4.091	0.637	0.021	2.89	0.191	0.008	0.058	Favourable
16	Qingyangshengenin	0.997	-4.483	0.365	0.083	-58.9	0.302	0.082	0.034	Favourable
17	Vincamone	1	-3.613	0.995	0.508	29.14	0.923	0.457	0.657	Unfavourable/Review
18	Pinolenic acid ethyl ester	0.998	-6.553	0.971	0.525	18.45	0.66	0.451	0.076	Unfavourable/Review
19	Nigerose	0.012	0.459	0.433	0	13.59	0.097	0.079	0.012	Favourable
20	Linoleic acid	1	-5.526	0.943	0.864	-14.84	0.873	0.262	0.048	Unfavourable/Review
21	10E,12Z-octadecadienoic acid	0.992	-5.112	0.811	0.043	17.36	0.247	0.089	0.068	Favourable
22	15(R)-15-Methylprostaglandin F2.alpha. methyl ester	0.999	-4.288	0.841	0.605	-21.36	0.521	0.112	0.129	Unfavourable/Review
23	Oleoside 11-methyl ester	0.144	-0.924	0.485	0.001	-6.51	0.038	0.121	0.133	Favourable
24	Oleic acid	0.998	-5.554	0.843	0.533	-12.57	0.487	0.179	0.052	Favourable
25	Linderane	1	-3.216	0.987	0.047	31.4	0.102	0.746	0.112	Favourable
26	Isopimaric acid	1	-5.287	0.819	0.167	-5.72	0.149	0.029	0.175	Favourable
27	Lupeol	0.999	-4.359	0.116	0.024	15.25	0.323	0.019	0.008	Favourable
28	Tricaprylin	0.999	-6.635	0.909	0.464	54.79	0.774	0.109	0.025	Favourable
29	Bicyclo-prostaglandin E1	0.996	-4.205	0.85	0.042	19.02	0.107	0.024	0.084	Favourable
30	3-Methoxylimaprost	0.993	-3.556	0.732	0.264	-20.9	0.125	0.136	0.154	Favourable
31	Hyodeoxycholic acid	0.96	-4.918	0.388	0.007	17.36	0.304	0.031	0.05	Favourable
32	Isoalantolactone	1	-4.09	0.888	0.101	1.28	0.146	0.257	0.176	Favourable
33	Picroside I	0.592	-1.981	0.495	0.021	-20.17	0.444	0.166	0.21	Favourable

34	Citrinin	0.999	-2.379	0.356	0.004	-30.15	0.004	0.197	0.156	Favourable
35	Ethyl Linoleate	1	-6.757	0.97	0.433	28.58	0.687	0.178	0.03	Favourable
36	Acid Violet 9	0.728	-3.03	0.123	0.063	158.09	0.701	0.167	0.147	Favourable
37	Quinupramine	0.999	-4.208	0.998	0.03	-15.34	0.984	0.277	0.39	Favourable
38	Brefeldin A	0.999	-2.014	0.751	0.129	-12.55	0.058	0.208	0.193	Favourable
39	4-(1-Phenylcyclohexyl)morpholine	1	-2.887	0.996	0.08	-0.96	0.521	0.193	0.181	Favourable
40	Hexamethylcyclotrisiloxane	1	-3.111	0.998	0	3.58	0.056	0.392	0.001	Favourable

BOILED-Egg plot

The BOILED-Egg model was employed to visualize and evaluate the passive gastrointestinal absorption and BBB permeability of the top five phytochemicals identified from *Wrightia tinctoria* through molecular docking. These included linoleic acid, oleic acid, β-sitosterol, cycloartenol, and lupeol, which showed the most favorable binding affinities to psoriasis-associated targets such as TNF-α, IL-6, and IL-17A. The BOILED-Egg plot revealed that linoleic acid and oleic acid are located within the yellow region, indicating a high probability of BBB permeability. In contrast, β-sitosterol, cycloartenol, and lupeol were positioned outside the yellow area, suggesting limited CNS exposure. All compounds displayed lipophilic properties (WLOGP > 5), which correlate with their predicted ability to permeate the stratum corneum, a critical factor in topical delivery

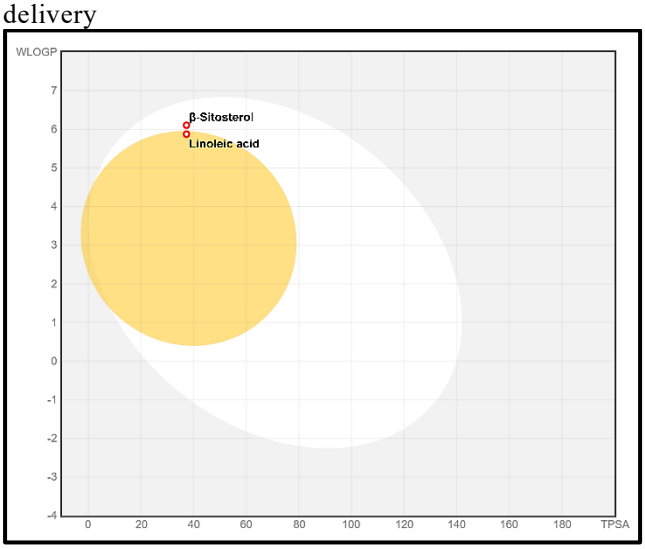

Figure 11: BOILED-Egg model depicting the predicted passive absorption and brain penetration properties of the two major fatty acids identified from *Wrightia tinctoria*, linoleic acid and β-Sitosterol

DISCUSSION

A network-based pharmacological investigation identified major inflammatory mediators as important nodes in psoriasis, underscoring the cytokine-driven pathophysiology. The major targets were IL-6, IL-17A, IL-1β, TNF-α, IL-22, IL-9, IL-10, TGF-β1, and the kinases JAK1 and TYK2. These data support the hypothesis that keratinocyte hyperproliferation is caused by a self-amplifying inflammatory loop involving IL-17A and TNF-α (13). Th17 cells in psoriatic lesions secrete IL-17A, IL-22, and IL-9, causing keratinocytes to release IL-6, TNF-α, and chemokines, perpetuating inflammation [13]. IL-9 has been linked to increased Th17 activity and angiogenesis in psoriasis [14], whereas IL-1β promotes immune cell infiltration and IL-17 synthesis. IL-22 causes epidermal thickening, while IL-10 and TGF-β1 are counter-regulatory processes that restore immunological balance within lesions.

The prevalence of JAK1 and TYK2 highlights the significance of intracellular cytokine signaling pathways in psoriasis. These kinases regulate disease-related cytokines, such as IL-6 and IL-10 via JAK1, and IL-23 and IFN-α via TYK2. The recent clinical approval of a selective TYK2 inhibitor for moderate-to-severe psoriasis [15] underlines the network's biological importance. Overall, the overlap between *Wrightia tinctoria* targets and key inflammatory pathways strengthens its therapeutic potential.

Molecular docking experiments confirmed that *W. tinctoria* phytochemicals can interact with a variety of psoriasis-related proteins. Among forty HR-LCMS-identified substances, β-sitosterol, lupeol, cycloartenol, linoleic acid, and oleic acid exhibited significant binding across several sites. These chemically diverse molecules—ranging from sterols and triterpenoids to unsaturated fatty acids—indicate a multitarget mechanism in which different chemicals preferentially bind to specific hub proteins. Key contacts were found at functionally relevant locations, such as cytokine interfaces and kinase regulatory or ATP-binding areas, indicating possible inhibitory effects. Previous *in silico* studies have shown high binding of *W. tinctoria*

elements to IL-17A and TNF-α [13]. Overall, the findings point to a synergistic, network-level mechanism rather than a single-target method of action.

In silico ADMET analysis revealed that the top-ranked compounds have physicochemical and safety profiles suitable for topical treatment. Topical psoriasis management benefits from the lipophilic qualities of sterols and triterpenoids like β-sitosterol and lupeol, which promote skin retention and reduce systemic exposure. Ex vivo investigations have demonstrated effective skin penetration of β-sitosterol [18], which aligns with our predictions. Linoleic and oleic acids, which are renowned skin penetration enhancers, also aid in dermal delivery and barrier restoration. Linoleic acid acts as a PPAR-α agonist in keratinocytes, leading to barrier normalization and anti-inflammatory effects [19].

Toxicity projections found no significant safety issues, and all lead chemicals are either food ingredients or widely used in topical preparations. Experiments show that β-sitosterol reduces epidermal hyperplasia and inflammatory cytokines in imiquimod-induced psoriasis while maintaining barrier integrity [18]. Lupeol suppresses TNF-α, IL-1β, and IL-6 while upregulating IL-10 and TGF-β1, promoting anti-inflammatory and tissue healing processes [20]. Fatty acids, such as linoleic acid, help to restore lipid composition and indirectly modulate immunological responses [19]. The traditional *Wrightia tinctoria* oil formulation has also been shown to be safe in repeated-dose animal trials [13].

Overall, the data imply that *W. tinctoria* has therapeutic effects by modulating pro-inflammatory cytokines, intracellular signaling kinases, and skin barrier function. This multitarget, synergistic approach is especially effective for psoriasis, a condition characterized by redundant and overlapping inflammatory processes. The findings offer mechanistic support for the traditional usage of *W. tinctoria* oil (Vetpalai thailam) and point to its possible development as a steroid-free topical therapy [13,16].

While the computational results are encouraging, they remain hypothesis-generating. It is critical to validate experimental findings using *in vitro* target-based assays, cell-based cytokine investigations, and in vivo psoriasis models. The next essential stages will be to investigate synergistic interactions between key drugs and optimize topical formulations, potentially using sophisticated delivery technologies. Overall, this study provides a compelling scientific foundation for the continued development of *Wrightia tinctoria* as a safe, multitarget phytotherapeutic for psoriasis therapy [13].

CONCLUSION

The current study provides a comprehensive computational insight into how *Wrightia tinctoria* can exert therapeutic effects against psoriasis. The network pharmacology analysis identified the key molecular drivers of psoriasis, and subsequent docking and ADMET evaluations suggested that multiple phytochemicals from *W. tinctoria* can favorably interact with those drivers and are suitable for topical delivery. These findings bridge traditional knowledge and modern science – validating the ethnomedical use of *W. tinctoria* and pinpointing the molecular basis for its efficacy. The phytochemical multitarget approach exemplified by *W. tinctoria* could represent a new paradigm in anti-psoriatic therapy, emphasizing restoring balance in the skin's immune network rather than inhibiting one pathway outright. Ultimately, while further laboratory and clinical studies are warranted to confirm these results, our work lays the groundwork for *developing W. tinctoria and its constituents as safe, multifaceted* anti-psoriatic agents, potentially fulfilling an unmet need for effective long-term topical management of psoriasis. Such plant-derived treatments, used either alone in mild cases or alongside conventional therapies in more severe cases, hold promise for improving patient outcomes and expanding the therapeutic arsenal against psoriasis.

Acknowledgement: The authors acknowledge the support received from JSS Academy of Higher Education and Research.

Conflict of interest: The authors declare no conflict of interest.

REFERENCE

1. Chakith MRS, Pradeep S, Gangadhar M, Maheshwari NC, Pasha S, et al. Advancements in understanding and treating psoriasis: a comprehensive review of pathophysiology, diagnosis, and therapeutic approaches. PeerJ. 2025;13:e19325. doi:10.7717/peerj.19325.

2. Schön MP. Adaptive and innate immunity in psoriasis and other inflammatory disorders. Front Immunol. 2019;10:1764. doi:10.3389/fimmu.2019.01764.

3. Sangeetha S, Hari A, Pattam S, Nihal P, Athira A. An updated review on Wrightia tinctoria (Roxb.) R Br. J Pharm Res Int. 2021;33(56A):234–44. doi:10.9734/jpri/2021/v33i56A33906.

4. Srivastava R. A review on phytochemical, pharmacological, and pharmacognostical profile of Wrightia tinctoria: adulterant of kurchi. Pharmacogn Rev. 2014;8(15):36–44. doi:10.4103/0973-7847.125528.

5. Li L, Yang L, Yang L, He C, He Y, Chen L, et al. Network pharmacology: a bright guiding light on the way to explore personalized precise medication of traditional Chinese medicine. Chin Med. 2023;18(1):146. doi:10.1186/s13020-023-00853-2.

6. Mo N, Zhou P, Liu F, Su H, Han L, Lu C. Integrating network pharmacology, molecular docking, and experimental validation to reveal the mechanism of Radix Rehmanniae in psoriasis. Medicine (Baltimore). 2024;103(43):e40211. doi:10.1097/MD.0000000000040211.

7. Yue Q, Li Z, Zhang Q, Jin Q, Zhang X, Jin G. Identification of novel hub genes associated with psoriasis using integrated bioinformatics analysis. Int J Mol Sci. 2022;23(23):15286. doi:10.3390/ijms232315286.

8. Pradeep S, Chakith MR, Sindhushree SR, Reddy P, Sushmitha E, Purohit MN, et al. Exploring shared therapeutic targets for Alzheimer's disease and glioblastoma using network pharmacology and protein–protein interaction approach. Front Chem. 2025;13:1549186. doi:10.3389/fchem.2025.1549186.
9. Pradeep S, Jain AS, Dharmashekara C, Prasad SK, Akshatha N, Pruthvish R, et al. Synthesis, computational pharmacokinetics report, conceptual DFT-based calculations and anti-acetylcholinesterase activity of hydroxyapatite nanoparticles derived from Acorus calamus plant extract. Front Chem. 2021;9:741037. doi:10.3389/fchem.2021.741037.
10. Prasad SK, Pradeep S, Shivamallu C, Kollur SP, Syed A, Marraiki N, et al. Evaluation of Annona muricata acetogenins as potential anti-SARS-CoV-2 agents through computational approaches. Front Chem. 2021;8:624716. doi:10.3389/fchem.2020.624716.
11. Pradeep S, Prabhuswaminath SC, Reddy P, Srinivasa SM, Shati AA, Alfaifi MY, et al. Anticholinesterase activity of Areca catechu: in vitro and in silico green synthesis approach in search for therapeutic agents against Alzheimer's disease. Front Pharmacol. 2022;13:1044248. doi:10.3389/fphar.2022.1044248.
12. Reddy P, Pradeep S, SM G, Dharmashekar C, D G, Chakith MR, et al. Cell cycle arrest and apoptotic studies of Terminalia chebula against MCF-7 breast cancer cell line: an in vitro and in silico approach. Front Oncol. 2023;13:1221275. doi:10.3389/fonc.2023.1221275.
13. Dayanand ND, Devi V, Kabbekodu SP, Amuthan A, SP B, Chinta R. Phytochemical and pharmacoinformatics analysis of a traditional antipsoriatic oil formulation for its potential against proinflammatory cytokines TNF-α and IL-17A. PLoS One. 2025;20(9):e0330939. doi:10.1371/journal.pone.0330939.
14. Midde HS, Priyadarssini M, Rajappa M, Munisamy M, Mohan Raj PS, Singh S, et al. Interleukin-9 serves as a key link between systemic inflammation and angiogenesis in psoriasis. Clin Exp Dermatol. 2021;46(1):50–7. doi:10.1111/ced.14335.
15. Armstrong AW, Gooderham M, Lynde C, et al. Tyrosine kinase 2 inhibition with zasocitinib (TAK-279) in psoriasis: a randomized clinical trial. JAMA Dermatol. 2024;160(10):1066–74. doi:10.1001/jamadermatol.2024.2701.
16. Sundarrajan S, Lulu S, Arumugam M. Deciphering the mechanism of action of Wrightia tinctoria for psoriasis based on systems pharmacology approach. J Altern Complement Med. 2017;23(11):866–78. doi:10.1089/acm.2016.0248.
17. Lomenick B, Shi H, Huang J, Chen C. Identification and characterization of β-sitosterol target proteins. Bioorg Med Chem Lett. 2015;25(21):4976–9. doi:10.1016/j.bmcl.2015.03.007.
18. Chang ZY, Chen CW, Tsai MJ, Chen CC, Alshetaili A, Hsiao YT, et al. Elucidation of structure–activity and structure–permeation relationships for the cutaneous delivery of phytosterols to attenuate psoriasiform inflammation. Int Immunopharmacol. 2023;119:110202. doi:10.1016/j.intimp.2023.110202.
19. Lin TK, Zhong L, Santiago JL. Anti-inflammatory and skin barrier repair effects of topical application of some plant oils. Int J Mol Sci. 2018;19(1):70. doi:10.3390/ijms19010070.
20. Beserra FP, Gushiken LFS, Vieira AJ, Bérgamo DA, Bérgamo PL, de Souza MO, et al. From inflammation to cutaneous repair: topical application of lupeol improves skin wound healing in rats by modulating cytokine levels, NF-κB, Ki-67, growth factor expression, and collagen distribution. Int J Mol Sci. 2020;21(14):4952. doi:10.3390/ijms21144952